Needle Insertion Test Using Navi-Robot and a CT Scanner

Mario Donnici, Giorgia Lupinacci, Paola Nudo, Michele Perrelli and Guido Danieli
DIMEG – Dipartimento di Ingegneria Meccanica, Energetica e Gestionale
Università della Calabria
Via Ponte Pietro Bucci, Cubo 46C – 87036 – Arcavacata di Rende (CS)
ITALY
danieli@unical.it http://www.chtsrl.com

Abstract: - The goal of this study was to validate the suitability of our robotic system, Navi-Robot, to guide percutaneous needle placement under computed tomography (CT) in order to achieve lower radiation exposure and a shorter procedure. The system consists of a six-degrees-of-freedom self-balanced arm, which allows the physician an accurate needle-insertion. The target and the needle entry points are selected by the surgeon on a desktop computer, that acquires DICOM images from the CT scan, and that, using software developed for this purpose, detects also the position of at least three radio opaque markers placed on the patient, and localized by the robot after CT scan. A first test was performed on a Plexiglas board; the accuracy achieved was measured as the distance between the needle tip and the target. The results of the in vitro experiment showed that the system is able to reach the target with an accuracy of 1.2 mm.

Key-Words: - Surgical Robots, Biopsy Needle Insertion, CT Images

1 Introduction

Surgical robots are becoming popular in the field of minimally invasive surgery especially for percutaneous needle insertion, which is a commonly used procedure in medical treatments such as: biopsies, brachytherapy, radio frequency ablation (RFA), cryoablation or chemotherapy. In this regard, using robotic surgery provides two important advantages: the increased precision of positioning and reduction of radiation exposure. The first one, resulting in significantly less pain, scarring and recovery time for patients, in addition to a shorter hospital stay. The second one is even more important since the quantities of radiation generated during these operations are not insignificant and the absorbed doses may predispose both the patient and the surgeon as well to the development of a variety of potentially devastating complications [1]. In this regard, several international organizations involved in establishing radiation safety guidelines are becoming increasingly concerned with this issue [2]. The risk is even higher for children because their growing tissue is more susceptible to ionization, and they have a longer life span to develop malignancies [3]. A number of specialized image-guided robots have been developed for ensuring patient and surgeon safety while providing imager compatibility.

Minerva (Swiss Federal Institute of Technology, Lausanne and Zurich) is a computer tomography (CT)-guided, multifunction neurosurgical robot [4], which is able to operate inside a CT gantry with longitudinal movement allowing cranial scans at any level. The physician using a remote control, can manipulate two instruments and the tool for automatic penetration of the tissue, skull, and meninges. A remote center of motion (RCM)-based prototype robot designed for needle alignment inside a CT gantry was developed by Siemens [5]. The system consists of a small radiolucent distal robotic system which allows an active needle orientation about a fixed location. For this application, a new CT fluoro-servoing algorithm was developed for targeting purposes and needle insertion was performed manually once the needle guide is in position.

The AcuBot robot [6] has been designed for X-ray guided percutaneous interventions and it uses revised PAKY and RCM modules while incorporating two newly designed components, and XYZ Cartesian stage and a passive S-Arm, mounted on a “bridge” frame. Studies demonstrate that this robotic system is significantly more accurate than a Computer-Assisted Navigation System [7]. Another CT-integrated system for interventional procedures was developed including preliminary experiments [8-10].

The goal of this paper is to describe the design and testing of a 6-DoF-needle driver prototype to demonstrate the proof-of-concept and to study its accuracy. Target registration is achieved using spherical markers placed on the patient’s body. A CT scanner allows to determinate the position of the

target in its frame of reference. Supplying then the scanner DICOM images to an algorithm, the spherical markers positioned on the patient are automatically recognized determining their position in the CT scanner frame of reference. It is now easy to create a new coordinate system based on the markers positions, in which the target position is determined. Next moving the robot in passive mode to touch the center of the hollow spherical markers on the patient, it is possible to compute the target coordinates in the robot frame of reference, hence aligning the needle to the desired penetration trajectory calculated by an algorithm specifically implemented for this purpose.

2 Materials and method

The robotic system, used to perform precision biopsy, is the Navi-Robot, a hybrid parallel/serial kinematic developed by the Department of Mechanical Engineering at University of Calabria in cooperation with Calabrian High Tech s.r.l. [11-12]. The Navi-Robot kinematic chain is composed of a planar four-bar-linkage with horizontal axis, which provides a single vertical degree of freedom, while a 3-DoF structure mounting parallel vertical axes, (SCARA like) is linked to the rod of the four-bar-linkage mechanism. To the fourth rotational DoF a fifth hinge with axis perpendicular to the fourth is linked, being the sixth again perpendicular to the previous, while the axes of the last three hinges meet in a single point, which behaves as a spherical hinge. A view of the 6-DoF arm's structure is show in Figure 1.

2.1 Calibration accuracy

The final position accuracy of the robot is mainly influenced by: kinematic inaccuracy (due to manufacturing and assembly errors in both actuated and passive joints), load deformation (due to external forces including gravity) and thermal deformation. In order to calibrate the robot, it is requested to reach some desired poses and the reached actual poses are measured. The terminal element of the calibration end-effector is a cube and on three faces of it, are placed 12 pins, equally spaced (Figure 2, Figure 3).
The axis of the end-effector connection tube passes through the center of the cube defining three different angles with respect to each face provided by pins.
The end-effector was designed to be placed in different known positions on a Plexiglas board provided by a series of holes on its surface. In particular, each 4-pins set of the cube can fit in 4 holes of the board forcing the robot to assume a different joints configuration for each face of the cube in contact with the board. Hence, during the calibration procedure, several poses of the end-effector were collected, registering the angles of the joints. These values are recorded together with the correspondent theoretic end-effector pose position.

Figure 1: Navi - Robot system: robotic system with 6 DOF

Figure 2: Terminal element of the calibration end effector

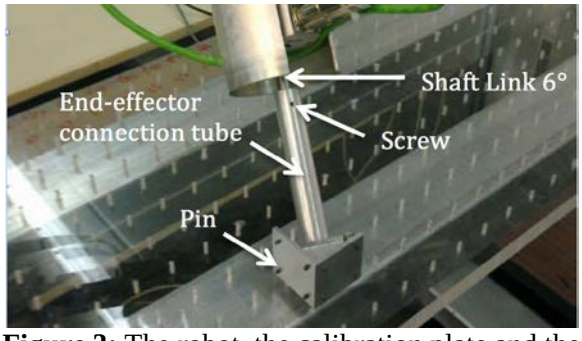

Figure 3: The robot, the calibration plate and the end effector during the calibration process.

To improve the calibration accuracy and to cover the whole working area with different end-effector orientation the measuring board was designed to have 360 insertion holes within the robot workspace. The calibration procedure was performed as follows: 180 poses were collected, for each of the 180 poses we evaluated the distance between the known end-effector positions with those estimated using the measured joint rotations and the evaluated structural parameter errors. Then, the exact robot geometry is estimated analyzing the difference between the desired and the reached poses. The average position error before calibration procedure was about 4.1 mm with standard deviation of 7.3 mm and 11.1 mm as maximum value. After the calibration, the average position error was -0.02 mm with a standard deviation of 0.3 mm and 0.9 mm as maximum value. In order to perform the biopsy, the end-effector used for the calibration was replaced by the end-effector bearing the needle and the marker described in section 2.2. Since even this end-effector is affected by geometric error due to manufacturing errors, a calibration procedure is required to compensate these errors by calculating a set of six error parameters denoting the end-effector geometry. A similar procedure to that previously described was executed. The tip of the needle was placed in known positions and we evaluated the distance between the known needle positions with those estimated using the measured joint rotations and the evaluated structural parameter errors. The average position error was 0.05 mm with standard deviation of 0.4 mm and 1.3 mm as maximum value. According to a definition from international standards (ISO 9283 [13]), we estimated the robot repeatability as:

$$R_p = l + 3\sigma = \pm 0.4mm \quad (1)$$

where $\boldsymbol{l}$ is the correlation factor, $\boldsymbol{\sigma}$ is a standard deviation and $\boldsymbol{R_p}$ is the repeatability range.

2.2 System components and needle insertion procedure

Besides the manipulator, in order to perform the needle insertion procedure, the position of the target visualized by using the CT scanner, must be known with respect the reference frame of the manipulator. To do so, three spherical markers, are rigidly attached, on the body's patient and on the needle driver. A Windows 7 personal computer is used to run the software for the user interface, which allows the surgeon to control each step of the needle insertion procedure described as follow:

1) First a CT scanning of the patient positioned on the CT table is obtained
2) The DICOM images are passed from the operator's workstation to the personal computer over an Ethernet connection.
3) The user interface software automatically determines the spherical markers position while allowing the physician to select the target point also defining the needle entry location,
4) The user interface computes the position of the target and entry point in the new frame of reference based on the markers position

Once the physician has chosen the correct needle path on the CT images, the robot registration process must start. This is done bringing the robot probe in passive mode to touch the center of the hollow spheres (M_1, M_2 and M_3) in any sequence pushing a pedal each time the position is reached, and leaving the robot arm in any position at the end of this process. Pushing again the pedal two times in short sequence commands the robot to reach the needle entry position orienting the needle in the right direction.
This requires us to determine the transformations between the various coordinate systems. To describe the position and orientation of a rigid body in three-dimensional (3-D) space, we attach a coordinate system to the object. We then describe the position and orientation of this coordinate system relative to the reference coordinate system. Touching the center of the spherical markers its coordinates in the robot coordinate system (RCS) are determined. Since the marker's as well as target and needle entry point positions are also known in the CTCS (CT coordinate system) it is now easy to transfer this information in the RCS.

2.3 Targeting computation

We define the needle coordinate system with respect to the robot reference frame as follow: the z-axis is located on the axis of symmetry of the end-effector frame, the x-axis is orthogonal to the plane of the frame and aligned to the alignment cylinder, and y-axis is calculated by the right-hand rule (Figure 4). Finally, the origin of the system is located at the tip of the needle. The needle axis is down along the x-axis and needle position coincides with the origin of the coordinate system. If the subscript denotes the object of interest and the superscript denotes the reference coordinate system, the needle position and orientation can be defined by a homogenous

transformation matrix ${}^{RCS}R_{init\_needle}$.

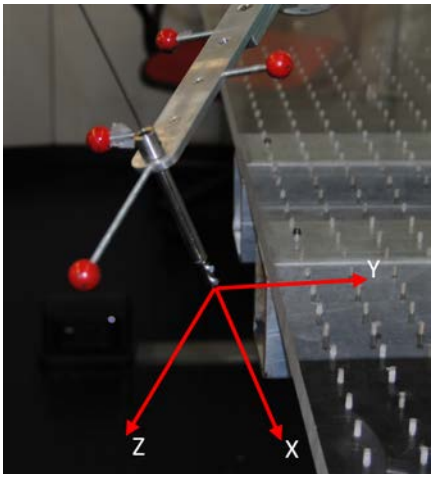

Figure 4: Needle system coordinates

Thus, knowing the 3D coordinates of the target and of the entry point reconstructed in the C-arm space, as well as the marker's coordinates, it is possible to introduce a new frame of reference, that will be named Patient Coordinate System (PCS) whose origin will correspond to the average of the marker's position, with z axis perpendicular to the plane containing the markers, x axis parallel to the line joining the two most distant ones, and y obtained with the right-hand rule. Clearly we will identify both a ${}^{CTCS}R_{PCS}$ and a ${}^{RCS}R_{PCS}$ respectively, and this will allow to easily pass from CTCS and RCS. In fact, knowing ${}^{CTCS}P_T$ and ${}^{CTCS}P_E$, we can map these points into the robot coordinates system as follow:

$$ {}^{RCS}P_T = {}^{RCS}R_{PCS} \times {}^{CTCS}R_{PCS}^{-1} \times {}^{CTCS}P_T \quad (2) $$

$$ {}^{RCS}P_E = {}^{RCS}R_{PCS} \times {}^{CTCS}R_{PCS}^{-1} \times {}^{CTCS}P_E \quad (3) $$

that allows using the entry point coordinate (Figure 5) (yellow marker) and target coordinates (green marker) to provide a new vector $\overrightarrow{ET}$, to which the needle is to be adjusted.

Having obtained the coordinates of the two points, we now need to compute the directional cosines in the RCS of the end effector's x axis, ensuring that the coordinates of point T in the needle CS will be positive, so that the robot will remain outside of the patient's body. A second condition was imposed on the y axis, to have zero component in the vertical direction (the z axis of the RCS).

Once x and y axes are established, and the origin of the needle CS is coincident with the entry point, it is possible to compute the set of joint parameters to be reached in order to position the end effector as requested, which requires the computation of the robot inverse kinematic.

$$ q = [q1, q2, q3, q4, q5, q6]^T \quad (4) $$

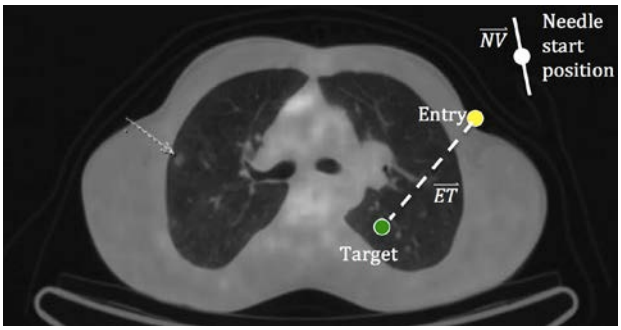

Figure 5: Needle path planning

Since at that moment the inverse kinematic of the robot did not take into account the geometric error, the vector q was corrected using the direct kinematic that contains the error parameters for geometric errors compensation. To do so, the vector q was used to evaluate the position of the tip needle at entry point ${}^{RCS}P_{E\_corr}$ and at the target point ${}^{RCS}P_{T\_corr}$ via direct kinematic. Thus the error can be minimized using the following equation (5):

$$ Err = \sqrt{\left({}^{RCS}P_{E_{corr}} - {}^{RCS}P_E\right)^2 + \left({}^{RCS}P_{T_{corr}} - {}^{RCS}P_T\right)^2} \quad (5) $$

Once the new set of joint parameters have been obtained, since after obtaining the marker's coordinates the robot was left in a relatively far from the patient position, also characterized by a set of joint parameters, it is now necessary to move the robot varying linearly the six parameters from initial to final position, and the system is ready for the biopsy.

Naturally the process seems very long, but once programmed and tested, it takes less than a second, from the moment in which the doctor presses twice the pedal to the moment in which the robot locks the brakes and moves to get ready for the biopsy.

3 Results

For the targeting procedure, the target consisted of radiolucent spheres 1, 2, 4 mm in diameter, placed on a screw locked in various positions of a Plexiglas board provided by three spherical markers,

resembling the body of the patient, and a CT scan of the object was performed (Figure 6).

Figure 6: CT scan of the rigid object simulating the patient

To perform the needle alignment and insertion the required translations and rotations were computed for each position. The needle holder, with the needle inserted up to the tip of the guide, was introduced into its position on the robot end-effector. With the system adjusted and locked to the specified positions, the needle was advanced through the needle guide to a pre-ticked position on the needle, specifying final needle depth (Figure 7). The targeting procedure was performed 24 times and the time to perform the procedure was about 3 min excluding the time necessary to import the CT images. The results are show in the Table 1.

Table 1: CT based targeting accuracy result

Sphere diameter [mm]	Success	Failure	Success rate
1	2	8	25%
2	12	0	100%
4	12	0	100%

4 Conclusions

The goal of this paper was the development of an image guided robotic system for needle-positioning procedures using a CT scanner. Such a system would aid the surgeon in inserting a needle into a tissue, reducing surgery time, surgery cost and patient-surgeon radiation exposure.

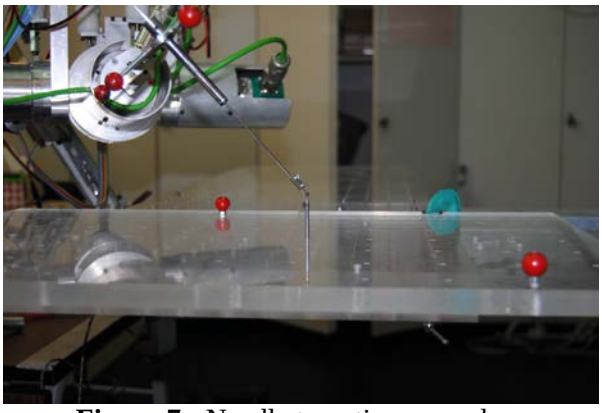

Figure 7: Needle targeting procedure

A number of error sources exist in the designed system. These error sources include errors originating from the calibration, point selection and repeatability of the robotic system. The decrease in targeting accuracy outside the calibration volume can also affect the accuracy of the system. Working inside the calibration volume is crucial in avoiding large targeting errors. This implies that the height of the target volume must be identified in the pre-surgery planning stage and taken into account during the calibration and targeting stage of the procedure. The mechanical of the robotic system with a mean of 0.678 mm was acceptable for the first prototype, however different mechanical solutions could be useful to achieve better robot accuracies and repeatability in order to restrict deflection of the axes of the joints, and other geometric errors. A number of improvements to the current robotic positioning system are possible. One would be the replacement of the manual insertion by an automated alternative such as the use another servo-or stepper motors which allows the needle to translate and rotate. This would increase procedure speed reducing the risk of needle deflection during the insertion, but would increase system cost.

References

[1] Butler, B. & Poelstra, K. A., Risks of Excessive Intraoperative Radiation.*Seminars in Spine Surgery*, 20(3), pp. 175-180, 2008

[2] Buls, N., Pagés, J., de Mey, J. & Osteaux, M., Evaluation of patient and staff doses during various CT fluoroscopy guided interventions. *Health Phys*., 85(2), p. 165– 173, 2003.

[3] Krille, L., Hammera, G. P. & Merzenicha, H., Systematic review on physician's knowledge about

radiation doses and radiation. *European Journal of Radiology*, p. 36–41, 2010.

[4] Hefti, J. L., Epitaux, M., Glauser, D. & Fankhauser, Robotic three-dimensional positioning of a stimulation electrode in the brain. *Comput Aided Surg*., 3(1), pp. 1-10, 1998.

[5] Loser, M. H. & Navab, N., A new robotic system for visually controlled percutaneous interventions under CT fluoroscopy. *Pittsburgh,PA, USA, Scott L. Delp, Anthony M. DiGoia, Branislav Jaramaz*, p. 887–896, 2000.

[6] Stoianovici, D. et al., AcuBot: A Robot for Radiological Interventions. *IEEE Transactions on Robotics and Automation*, 19(5), pp. 927-930, 2003.

[7] Pollock R., P. Mozer, T. J. Guzzo, J. Marx, B. Matlaga, D. Petrisor, B. Vigaru, S. Badaan, D. Stoianovici, et al., Prospects in Percutaneous Ablative Targeting: Comparison of a Computer-Assisted Navigation System and the AcuBot Robotic System. *Journal of Endourology*, Volume 24, Number 8, Pp. 1269–1272, August 2010

[8] Yilun Koethe & Sheng Xu & Gnanasekar Velusamy & Bradford J. Wood & Aradhana M. Venkatesan, Accuracy and efficacy of percutaneous biopsy and ablation using robotic assistance under computed tomography guidance: a phantom study, *Eur Radiol* (2014) 24:723–730 DOI 0.1007/s00330-013-3056-y

[9] F. Roser, M. Tatagiba, G. Maier, Spinal robotics: current Applications and Future Perspectives. N*eurosurgery* 72:A12–A18, 2013

[10] R. Seifabadi, S. Song, A. Krieger,N. B. Cho, J. Tokuda, G. Fichtinger, I. Iordachita, Robotic system for MRI-guided prostate biopsy: feasibility of teleoperated needle insertion and ex vivo phantom study. *Int J CARS* 7:181–190 DOI 10.1007/s11548-011-0598-9, 2012.

[11] Danieli G. Measuring open kinematic chain able to turn into a posizion robot. *European Patent* EP1843876, England, France, Germany, Italy. 2009

[12] Perrelli M., Nudo P., Donnici M., Gatti G., Colacino FM., Pace C., Danieli G., Navi – Robot, a multipurpose robot for medical application.,No 4(41), *Problem of Mechanics*, pp. 22-33, 2010.

[13] "ISO 9283 Manipulating Industrial Robots – Performance criteria and Related Test Methods".*International Standards Organization*. 1998.